

THIRTEENTH EUROPEAN ROTORCRAFT FORUM

<sup>6.12</sup>  
Paper No. 99

PITCH-FLAP FLUTTER INSTABILITY OF A SWEPT-TIP MODEL ROTOR BLADE

W R Walker  
C Hatch

Royal Aircraft Establishment  
FARNBOROUGH, England

8-11 September 1987  
Arles, France

ASSOCIATION AERONAUTIQUE ET ASTRONAUTIQUE DE FRANCE

Copyright

©

Controller HMSO  
London 1987

detailed investigation of the instability to be carried out, however, the rotor was transferred to a second rig which had instrumentation more appropriate to examining the instability. This particular rig used only a single blade, the other two being replaced by balance weights (Fig 3). Excitation is achieved by means of an electromagnetic shaker located above the rotor head and rotating with it. The oscillatory load is transmitted by a suitable linkage to a point at the root of the sweep/post cone element. This enables the blade to be excited in flap or lag depending on the linkage used.

The load is measured by means of a force cell at the point of attachment to the blade. The blade response is measured by means of strain gauges mounted along the blade and on the flexures. Gauges on the flapping elements and swept links are used to monitor the loads, to ensure safety and prevent damage to the rig. All the various signals are first pre-amplified at the rotor hub and then passed through slip rings to an HP5423A signal analyser for processing. Since both the input to the blade and its response are measured in the rotating frame, the frequency response functions may be analysed directly to provide frequencies and dampings of the rotating modes. Thus, no modifications to the response functions are necessary to eliminate the rotational frequency content, as they would be if fixed frame measurements were taken. The response analysis is conducted using the PAPA program<sup>5</sup> developed at RAE. Fig 4 illustrates the test configuration and the data collection procedure.

Initially, non-rotating modes were excited to provide data for assessing predictions in the least complicated theoretical case. This enabled the most appropriate representation of the secondary load paths to be identified, and also allowed the most suitable forcing direction and strain gauge measurement position to be determined for each mode. In all cases, the modes were excited by random noise, band limited to an appropriate frequency range about the mode natural frequency. The rotor speed was then increased in equal increments to a level about 10% below the expected flutter speed. The speed was further increased in finer increments as the flutter speed was approached. Because the data were analysed off-line, an exact indication of the flutter speed could not be obtained as the test was being run. However, the simple one degree of freedom curve fitter, available in the on-line analyser used to collect the data, was used to obtain an indication of the onset of instability. The onset of instability was also marked by an increased vibration level in the strain gauge signals and by a distinct change in tone of the noise produced by the rotor.

The Nyquist plots produced are entirely conventional, save for spikes which occur at integer multiples of rotational frequency (Fig 5). These are assumed to arise from background aerodynamic forcing. Their retention in the Nyquist plot analysis introduces errors in the derived mode frequencies and dampings. Before analysis, therefore, each spike is removed by interpolating the data linearly across the spike's base. It is intended in future tests to examine more closely the cause of these spikes to see if they can be eliminated at source, by first measuring the blade's response in the absence of forcing and then subtracting this from any subsequent forced response measurements. For the present, however, it is considered that the analysis procedure outlined above provides results to a suitable accuracy.

A series of Nyquist plots showing the coalescence of two modes as instability is approached is depicted in Figs 6, 7 and 8. Normal modes are represented in the Nyquist plane as circles, with the natural frequency at the point where the rate of change of response with frequency is greatest. An indication of the damping is given by the separation of the data points, a close spacing representing a high damping. Fig 6 shows two well separated modes with a typical level of structural damping. As the rotor speed increases, the overall level of aerodynamic damping increases, while the two modes approach each other in frequency to produce the cardioid plot of Fig 7. Finally, on the threshold of instability, the mode about to become unstable dominates the plot, with little evidence of there being a second mode present (Fig 8). The higher level of damping of the second mode is difficult to assess in these circumstances and is generally not quoted in the results that follow.

### 3 BLADE STABILITY COMPUTER PROGRAM

A new computer program for assessing rotor blade stability in hovering and axial flight has recently been developed at RAE. Programs available previously within the UK required as input the normal modes of the blade in a vacuum. It was found, however, that as parameters were varied, it was usually necessary to recalculate the modes in order to obtain sufficiently accurate results of stability boundaries. This was a time-consuming process.

The aim of the present program is to provide a direct analysis capability. Thus the full equations of motion, including the aerodynamic terms, are

# PITCH-FLAP FLUTTER INSTABILITY OF A SWEPT-TIP MODEL ROTOR BLADE

by

W R Walker  
C Hatch

Royal Aircraft Establishment  
Farnborough, England

## ABSTRACT

A joint theoretical and experimental investigation into the pitch-flap flutter of a swept-tip model rotor blade is described. The blade tip is swept aft to give a rearward shift of the centres of pressure and mass of the type that could be beneficial in the aeroelastically tailored blade concept. The form of the flutter is identified, as are the parameters which influence it most, and the means used to control the flutter are described.

## 1 INTRODUCTION

In recent years, there has been growing interest in the helicopter community in the concept of aeroelastic tailoring of helicopter rotors. The aim is to incorporate extra coupling effects into a blade's design which modify its response characteristics and so may be used to maximise a rotor's performance or minimise its vibration. One possibility is to incorporate a swept back blade tip with its centre of pressure and centre of mass behind the shear centre of the major part of the blade. If combined with appropriate design parameters, eg stiffnesses and twist, it may be possible to produce a beneficial aeroelastic response.

As a first step to understanding the problems involved, a model rotor has been built at RAE with swept-tip blades designed deliberately to give an appreciable offset of centre of pressure and mass. Such offsets were of course carefully avoided in the design of the swept tips investigated on the RAE Puma<sup>1</sup> and in the design of the BERP tip<sup>2</sup>. The model rotor blades (Fig 1) thus have no leading-edge extensions and are sharply swept back at 20° over the outer 12% of the rotor radius. The aim, initially, is to ensure that loads and performance programs currently available at RAE can predict the behaviour of such rotors. Studies conducted at the blade design stage indicated that the added couplings

would not cause instability but, when the rotor was first spun, pitch-flap flutter was encountered at just below the rotor normal operating speed.

This paper describes the subsequent experimental and theoretical investigations that were carried out in order to understand and avoid the flutter. The experimental rig is described, as is the blade stability program, recently developed at RAE, which is used to obtain the theoretical results. It is found that the flutter involves the interaction of modes of a higher order than normally associated with pitch-flap instability. However, conventional techniques of flutter suppression, by mass balancing and increased torsional stiffness, are still found to work. A solution is identified which allowed the rotor to reach its design speed with sufficient margin for safety, and thus enabled it to complete wind tunnel tests over a full range of forward speeds.

## 2 ROTOR EXPERIMENT

The rotor model used for this investigation is that developed for the 24ft wind tunnel at RAE<sup>3</sup>. The rotor is dynamically scaled, is 3.6m in diameter and has a normal operating speed of 600rpm. The blades are composed of a central carbon fibre reinforced plastic spar, embodied in a rigid foam aerodynamic fairing and covered by a thin glass fibre reinforced plastic skin<sup>4</sup>. This form of blade construction was chosen to enable representative mode frequencies to be obtained. Over its outer 12%, the blade is swept aft at an angle of 20°. No mass balancing is incorporated over this region, with the result that construction limitations caused the section CG to be placed 22mm behind the  $\frac{1}{4}$ -chord over the whole of the swept region. Inboard, however, some mass balancing is introduced, sufficient to ensure that the CG of the inboard sections is forward of the local  $\frac{1}{4}$ -chord by 3mm. The overall effect is to balance the blade as a whole in pitch about the inboard  $\frac{1}{4}$ -chord line. The initial twist of each blade is 4.4°/m and, throughout the experiment, a collective pitch of 12.7° was maintained. The blade chord is 0.14m and the aerofoil section is RAE 9642.

The blades are mounted on a dual load path hub, as shown in Fig 2. The essential features of the hub are flapping elements which do not carry the blade centrifugal loads, elastomeric pitch bearings and elastomeric lag dampers.

The instability was first encountered on the three-bladed rotor mounted on the wind tunnel rig at just below the rotor normal operating speed. To enable a

integrated directly. Because the equations are nonlinear, the steady state must first be determined by means of a perturbation procedure. The equations are then linearised about this position and the transient response found. The advantage of a direct approach is that only the complex frequency of the unstable mode need be calculated. Frequencies of other modes irrelevant to the problem in hand need not be determined, neither need the mode shapes, which require a more refined treatment if they are to be obtained to a commensurate accuracy.

The equations of motion are developed in Ref 6. They apply to a curved and twisted blade, and include the effects of cross-stiffness introduced by, say, a fibre composite construction. The derivation of stiffness coefficients for thin-walled orthotropic cylinders is provided by Mansfield and Sobey<sup>7</sup>. These coefficients, in effect, must be modified slightly in the presence of a high tensile load and pre-twist. This is undertaken in Ref 6, in a manner similar to that of Hodges<sup>8</sup>. The displacement formulation and, in particular, the second order definition of blade section orientations, follows that of Hodges and Dowell<sup>9</sup>. Warping restraint and transverse shear are ignored.

Aerodynamic lift, drag and pitching moment data are interpolated for a variety of aerofoils over a range of Mach numbers. The simple momentum balance equation is used to determine the downwash across an annulus, but allowance is made for the possible windmill brake flow state, which may arise at high axial velocities. This allows the characteristics of tail rotors in high cross-winds to be evaluated. Three-dimensional aerodynamic effects are not treated, tip relief being incorporated by means of an empirical tip loss factor. No treatment of dynamic downwash is provided.

The equations are solved by a transfer matrix technique and are integrated from tip to root by a second order integration method. Secondary load paths may be incorporated, but only using simple representations at present. Application of the root boundary conditions yields a frequency equation, the complex roots of which are interpolated by a quadratic fit procedure.

Because the blade equations of motion are treated in their entirety, the computer program may determine not only blade stability, but also rotor performance and loading in axial flight. In addition, the Coriolis, structural damping and aerodynamic terms (either before or after steady state calculation) may be eliminated if desired, thus enabling normal modes in a vacuum to be

determined. The program has been formulated to allow, at a later date, the inclusion of hub impedance effects arising from both the fuselage and the remaining rotor blades. This will be achieved by modifying the boundary conditions for a single blade, and will allow calculations of air and ground resonance to be made, as well as permit the effects of hub impedance on individual blade stability to be assessed.

#### 4 COMPARISON OF THEORETICAL AND EXPERIMENTAL RESULTS

The frequencies of the blade modes in a vacuum are depicted in Fig 9 for the basic blade configuration. Coriolis terms are retained, as are the aerodynamic loads which determine the steady state. It is found that the modelling of the root region is critical. The secondary load path, in particular, cannot be modelled simply as a spring to earth. A simple representation as a torsion spring with an appropriate inertia for the bearing housing has been used here, but clearly a more detailed representation is required to avoid the empiricism involved in selecting torsion spring location. It is also found important to include the shear stiffness of the root elastomer. Although high, this has significance in determining lag mode frequencies.

It may be seen from Fig 9 that the order of the non-rotating modes is 1F, 1L, 2F, 3F, 1T, 2L. The first torsion mode would appear to have a frequency sufficiently high to preclude its coupling with another mode to produce an instability. However, the swept tip generates modes which are far from 'pure', and there is, in fact, a significant torsional component in the third flap mode (as there is third flap in the torsion mode). It is this which combines with the second flap mode to produce the instability. The interaction, while being conventional in its involving blade pitch and flap, is unconventional and contrary to normal fixed-wing experience, for instance, in that higher order modes are involved. The implication is that it is the tip region of a rotating blade that is most influential in determining its aeroelastic characteristics.

When the aerodynamic loading is added, the frequencies and dampings of the modes of interest are as depicted in Fig 10. As may be seen, the theoretical and experimental results generally compare well. The zero damping of one of the modes indicates the onset of instability at just below the rotor design speed of 600rpm. The damping of the second mode is not depicted in the experimental case, due to difficulties in identifying a highly damped mode at frequency coalescence

with a lowly damped one. As far as the theoretical results are concerned, damping levels are found to depend significantly on the tip loss factor chosen. It is assumed here that the aerodynamic lift and pitching moment fall linearly to zero over the outer 6% of the blade.

The modes associated with these complex roots are themselves complex, Fig 11, with little evidence of third flap content. That mode which goes unstable, either theoretically or experimentally, has a relative phase of flap and torsion at the blade tip such that there is a positive pitch as the blade passes through the flapping equilibrium point. This is the condition for energy input from the airflow. The unstable mode, however, may emanate from either of the two participating modes, and can switch from one to the other on the slightest of configuration changes. In some cases, such as that of Fig 10, the unstable mode emanates from a different mode in theory to that found in practice. The shape of the unstable complex mode, however, always takes the form described above. This finding is common in situations of frequency coalescence, and has been observed and explained by Niblett<sup>10</sup>.

Since the flutter occurs between the flap and torsion motions, it is to be expected that mass balancing might be instrumental in curing it. The results, however, are not as encouraging as hoped. Adding mass to the leading edge of the swept tip places the mass behind the  $\frac{1}{4}$ -chord of the rest of the blade and this is detrimental to stability. Placing the mass immediately inboard of the swept portion is best (Fig 1). With 120gm of lead bonded over the 10cm immediately inboard of the crank, stability margins are improved to those of Fig 12. This mass represents the maximum that can be accommodated within the space available along the blade leading edge. However, the improvement in stability was not felt to be sufficient to cater for the overspeed case in the practical situation. The poor response to mass balancing is possibly due to the mass being placed too close to the node of the second flap mode, thus reducing its decoupling effect with torsion. Mass placed further inboard has little influence, and indeed can be slightly detrimental if placed inboard of the second flap mode node, since the relative phase of flap and torsion is then different.

Enhancing the torsional stiffness has significantly more impact (despite both modes being notionally flap). This was achieved experimentally by bonding layers of  $\pm 45$  carbon fibre along the blade length (Fig 1). With the torsional stiffness doubled, mode frequencies and dampings become as depicted in Fig 13.

The instability has been removed to a safe distance. Such a solution, however, is contrary to the concept of a compliant rotor. Accordingly, a compromise solution was examined with a modest 34% increase in torsional stiffness and 40gm of added mass. The results for this configuration are depicted in Fig 14 and indicate an acceptable degree of flutter suppression. By interpolating these various results, it was considered that an increase in torsional stiffness of 16% and an added mass of 80gm offered the best compromise, providing sufficient margin of safety for wind tunnel tests whilst retaining maximum flexibility in the blade. Blades have been built to around this specification and have now completed tests over a full range of forward speeds in the RAE 24ft wind tunnel.

One further observation must be made which as yet remains unexplained. When the instability was first encountered, it occurred on the wind tunnel rig with a full set of three blades. Subsequent tests were carried out on an alternate rig, which had a stiffer tower and could only accommodate one rotor blade. Flutter was detected on this second rig at around a 5% greater tip speed. It is not known as yet whether this is due to rig dynamics, to the number of blades, as they influence each other through the wake, say, or to differences in the control circuits. Initial theoretical studies indicate so far that neither transient wake effects nor changes in the wake due to the number of blades have sufficient influence to produce the discrepancy. Certain refinements to the theory are currently in progress, however, to include the interactive effects of blades across the hub, for instance, and these may help to shed some light on the matter. Further, more detailed experimental investigations are also planned.

## 5 CONCLUSIONS

A joint theoretical and experimental investigation has been carried out into a pitch-flap flutter instability encountered on a swept-tip model rotor blade. Results from the two approaches compare well. They indicate that the instability involves the interaction of the second flap mode and the torsion component of the third flap mode. The flutter may be cured by mass balancing or by enhancing the torsional stiffness. The former has limited effect, and the latter is counter to the concept of a torsionally compliant rotor. In the practical case considered here, a combination of the two was used to provide the degree of stability required.

It is found that the aerodynamic representation of the tip region and the dynamic representation of the root region are both critical to obtaining good results. Refinements to the theory are planned, to include hub motions and a better representation of secondary load paths. It is hoped that this will help to explain the 5% change in stability boundary found on moving from the three-bladed to the one-bladed rig.

#### Acknowledgment

The authors wish to acknowledge A.R. Lee for his assistance throughout the experimental tests.

## REFERENCES

- 1 M.J. Riley  
J.V. Miller Pressure distributions on a helicopter swept tip from flight tests and from calculations.  
Ninth European Rotorcraft Forum, 1983
- 2 R.E. Hansford Rotor load correlation with the ASP blade.  
American Helicopter Society Forum, 1986
- 3 J.T. Cansdale  
R.J. Marshall  
P.A. Thompson Tests on a new dynamically scaled model rotor in the RAE 24ft wind tunnel.  
Tenth European Rotorcraft Forum, Paper No.98, 1984
- 4 A.R. Lee A method for the manufacture of model helicopter rotor blades with torsional stiffness representative of full scale.  
RAE Technical Report 85094, 1985
- 5 J.C. Copley Numerical analysis of vector responses.  
RAE Technical Report 80135, 1980
- 6 W.R. Walker Equations of motion for a fibre composite helicopter rotor blade.  
RAE Technical Report, to be published
- 7 E.H. Mansfield  
A.J. Sobey The fibre composite helicopter blade.  
RAE Technical Report 78139, 1978
- 8 D.H. Hodges Torsion of pretwisted beams due to axial loading.  
Journal of Applied Mechanics, Vol 47,  
pp 393-397, 1980
- 9 D.H. Hodges  
E.H. Dowell Nonlinear equations of motion for the elastic bending and torsion of twisted non-uniform rotor blades.  
NASA TN D-7818, 1974
- 10 L.L.T. Niblett A graphical representation of the binary flutter equations in normal co-ordinates.  
RAE Technical Report 66001, 1966

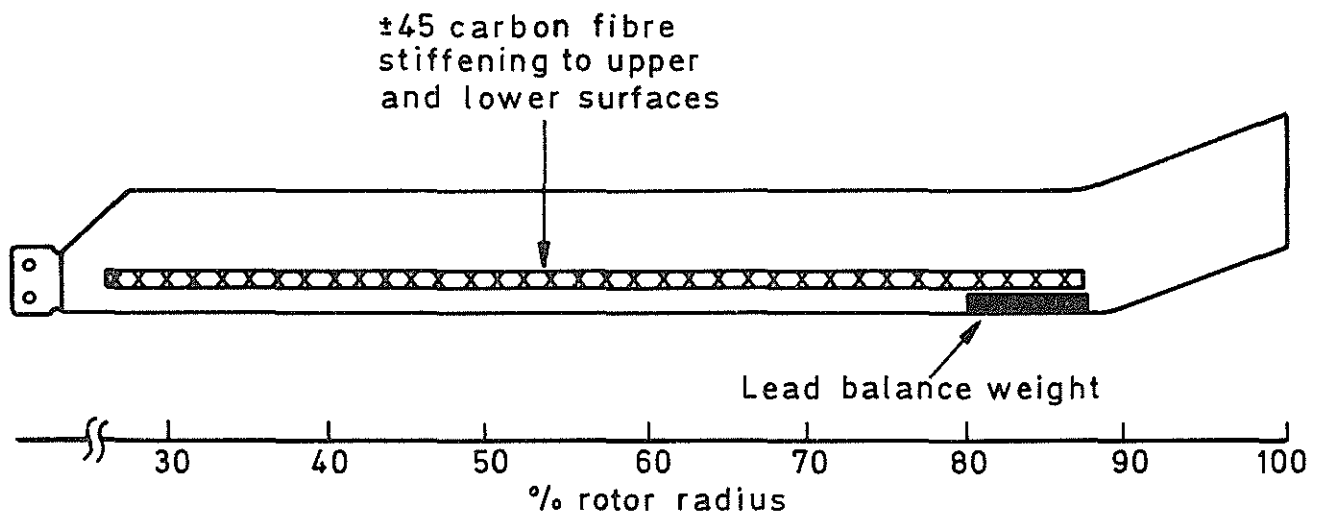


Fig 1 Model blade showing planform and structural modifications

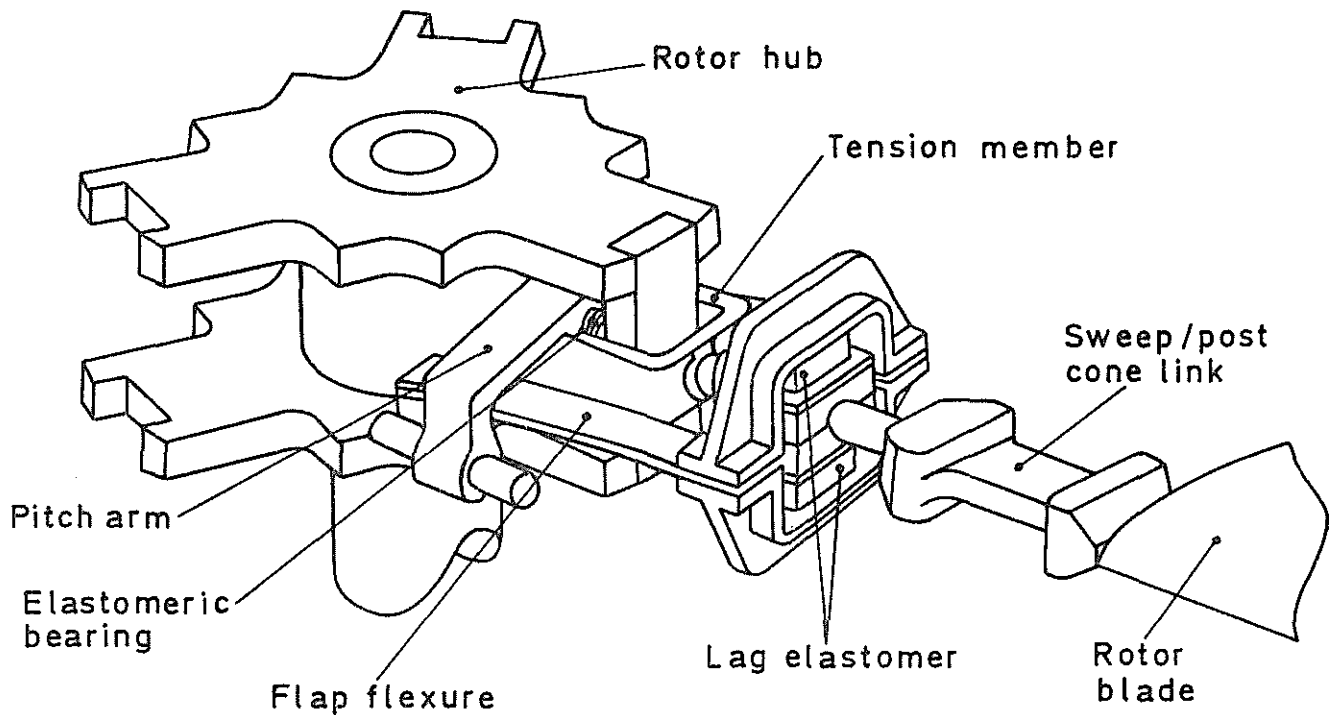
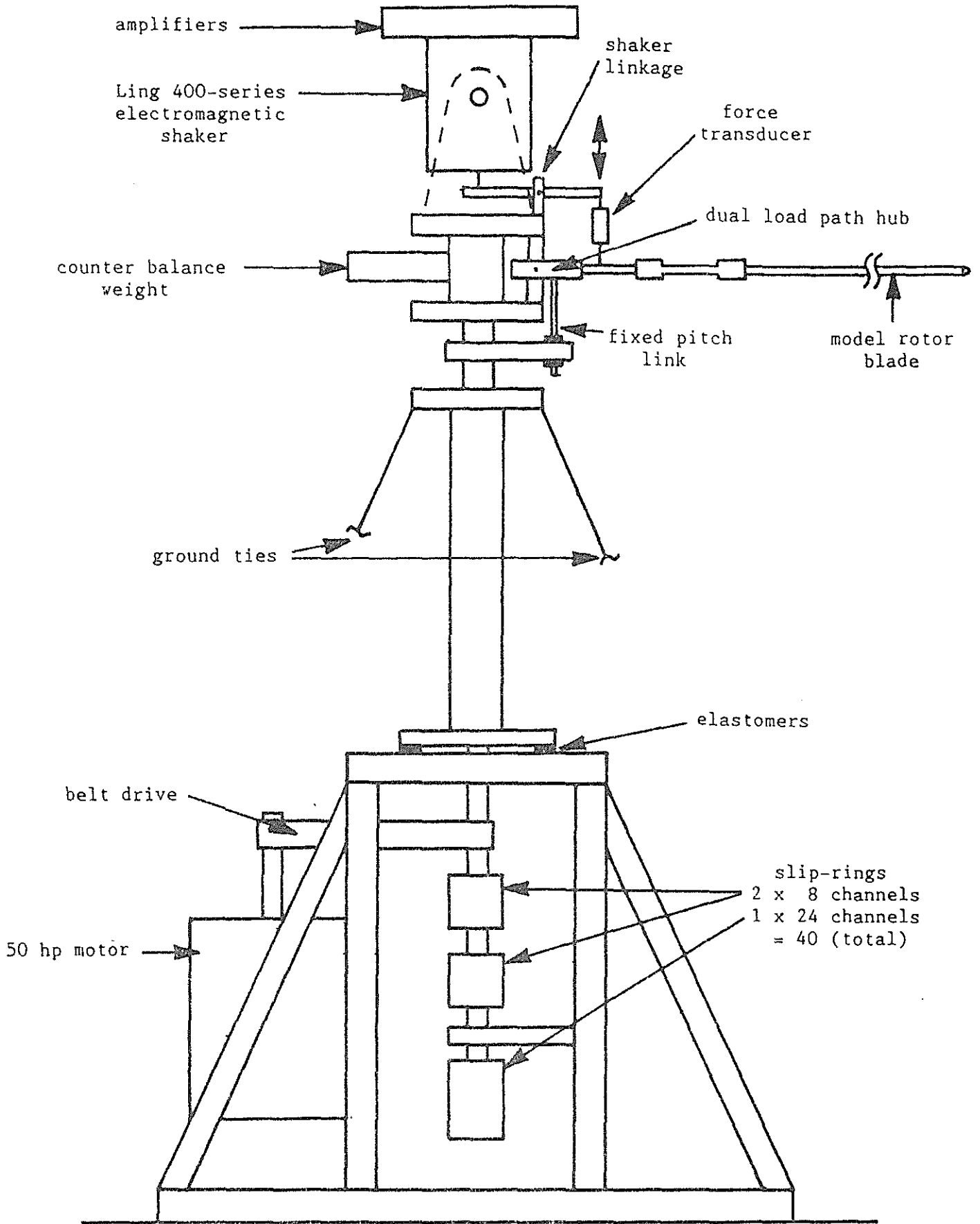


Fig 2 Dual load path (DLP) rotor model



Not to scale

Fig 3 RAE single-blade spinning tower

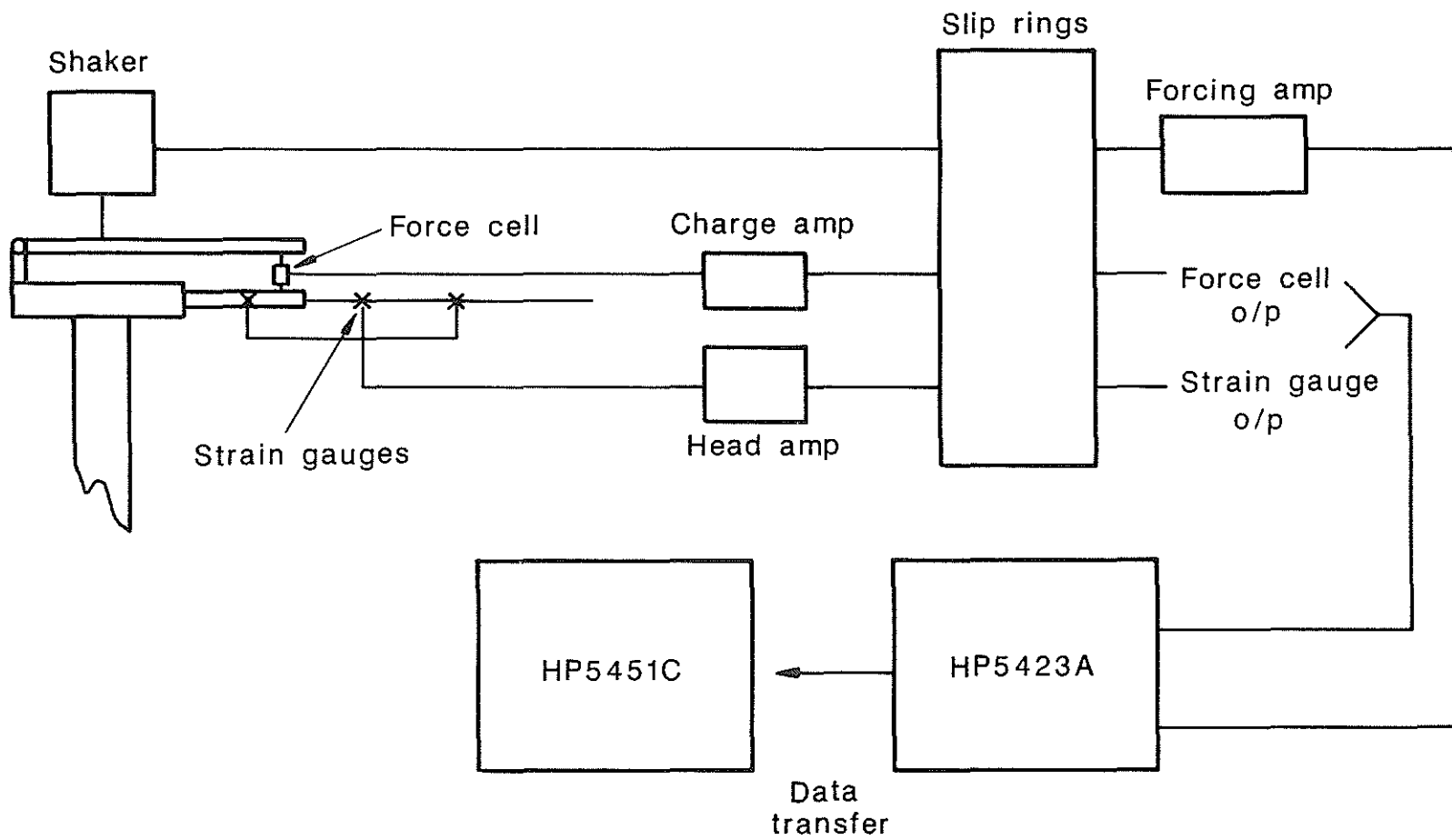


Fig 4 Schematic test configuration

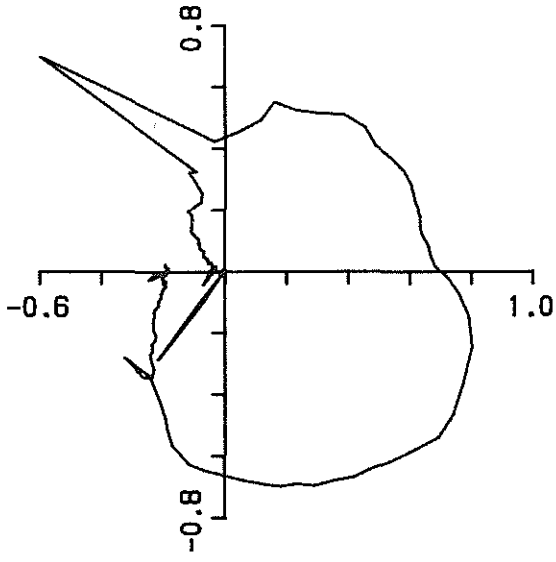


Fig 5 Nyquist plot showing spikes at multiples of rotational frequency

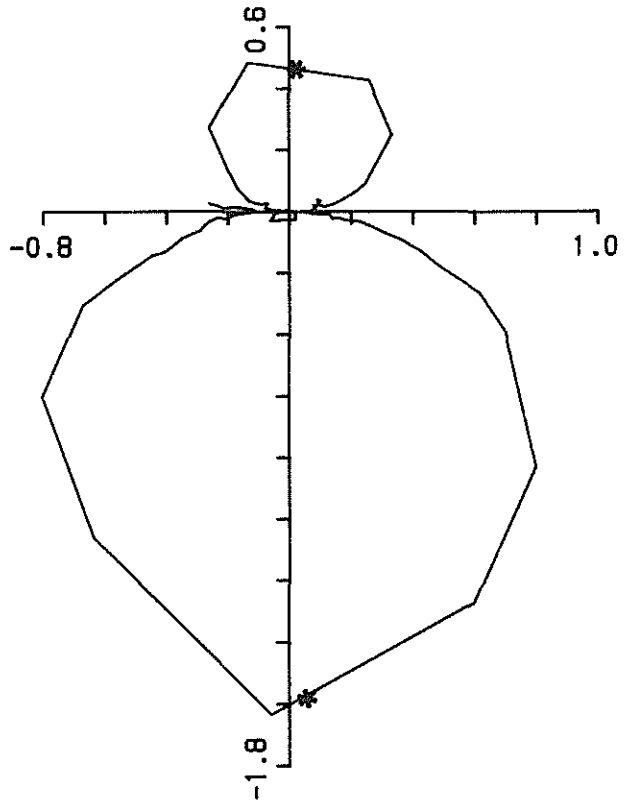


Fig 6 Nyquist plot for two modes, non-rotating

\* modal frequency

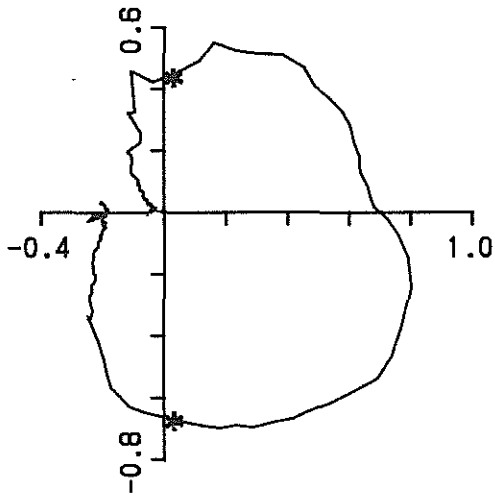


Fig 7 Nyquist plot for two modes at 500 rpm

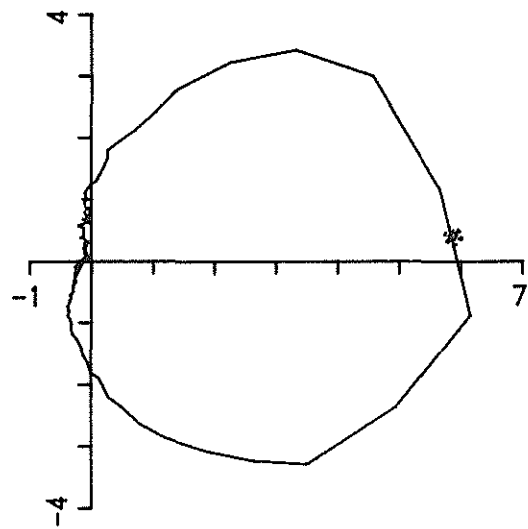


Fig 8 Nyquist plot for two modes at 600 rpm

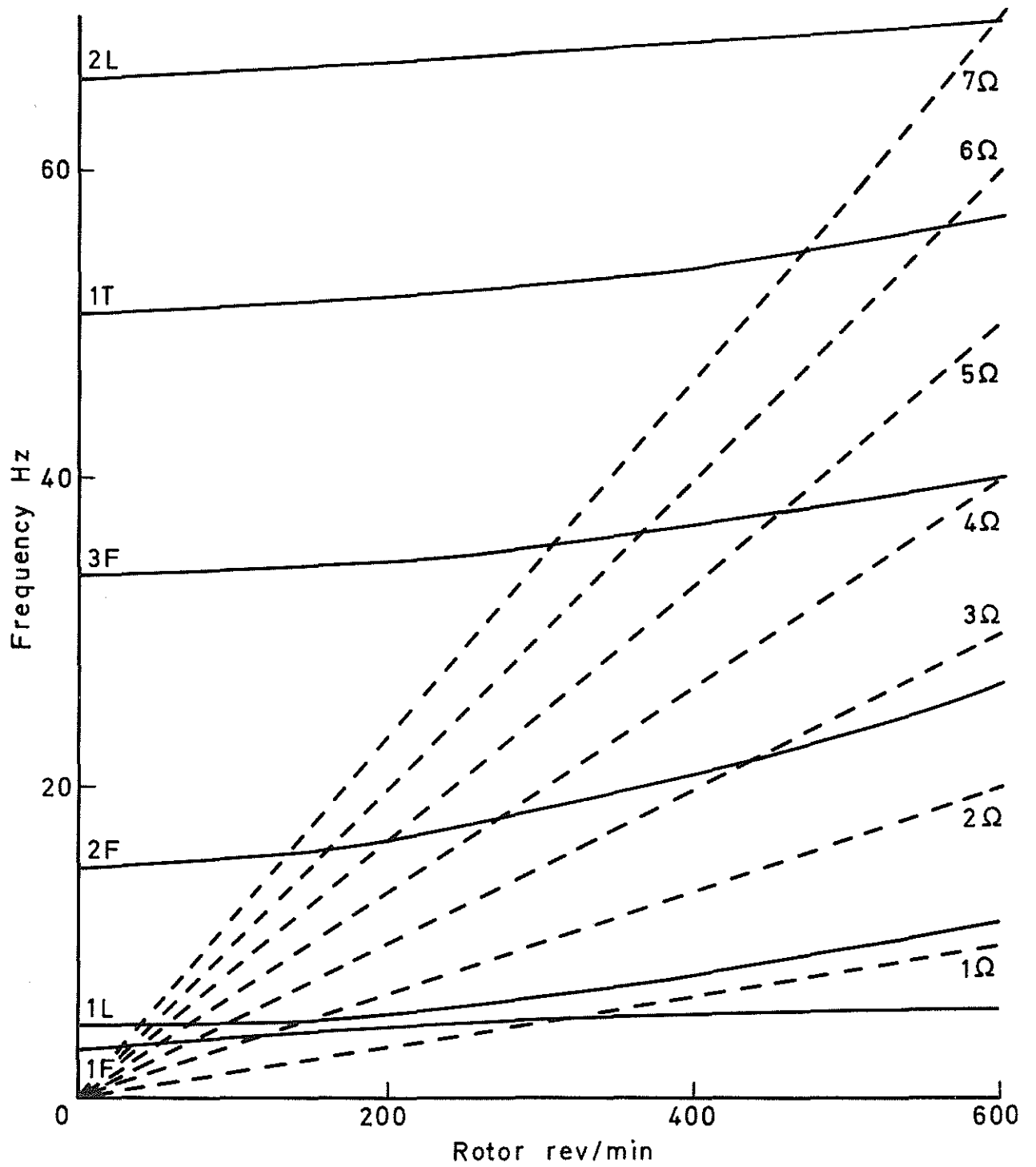
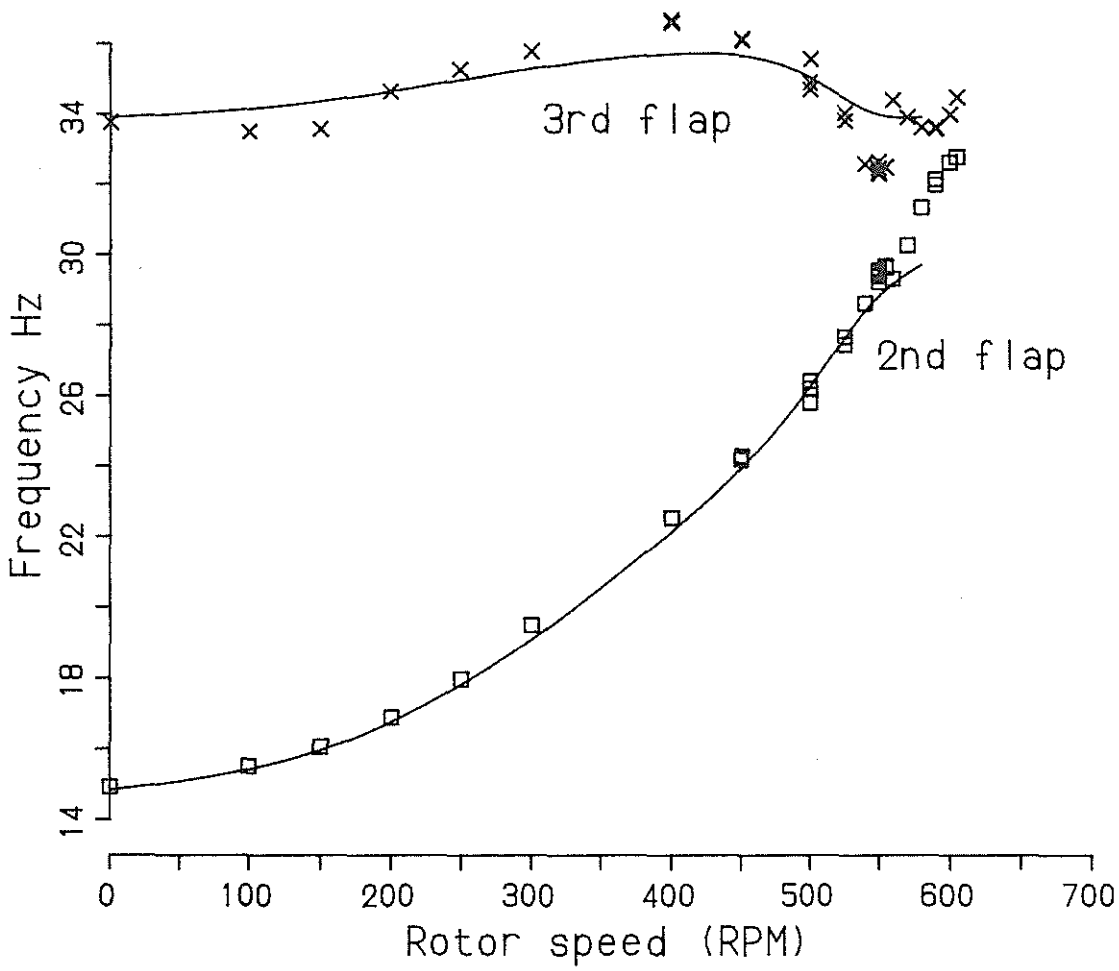


Fig 9 Blade mode frequencies in vacuum



experimental data points :  $\square$  2nd flap  
 $\times$  3rd flap

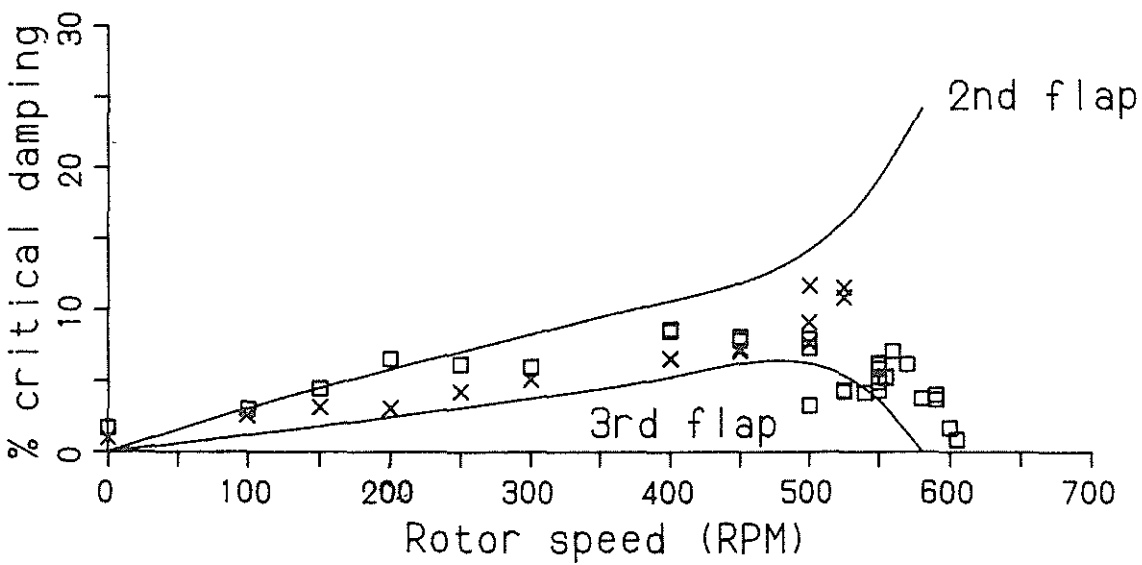


Fig 10 Modal frequencies and dampings for basic swept-tip blade

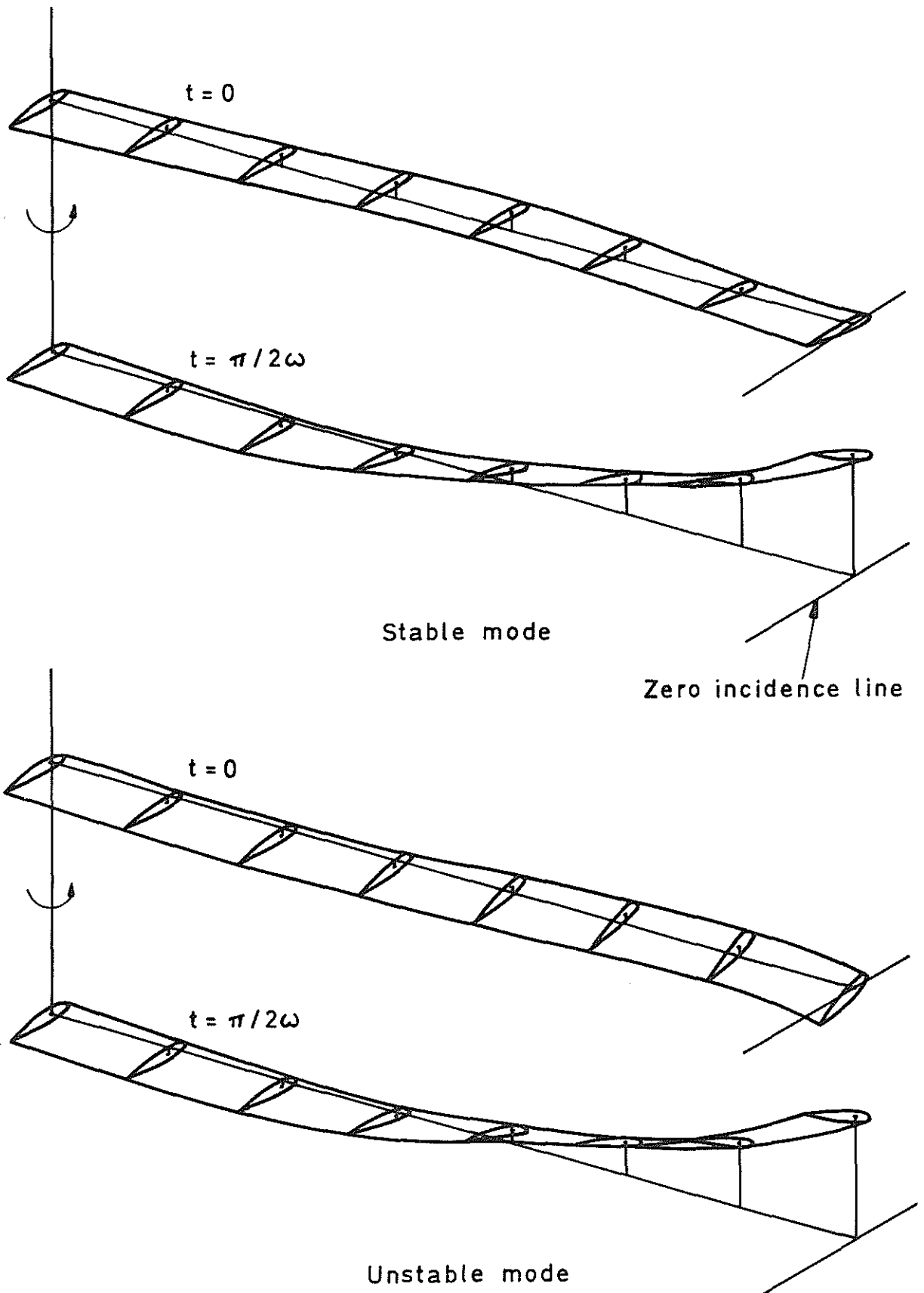


Fig 11 Complex shapes of the interacting modes

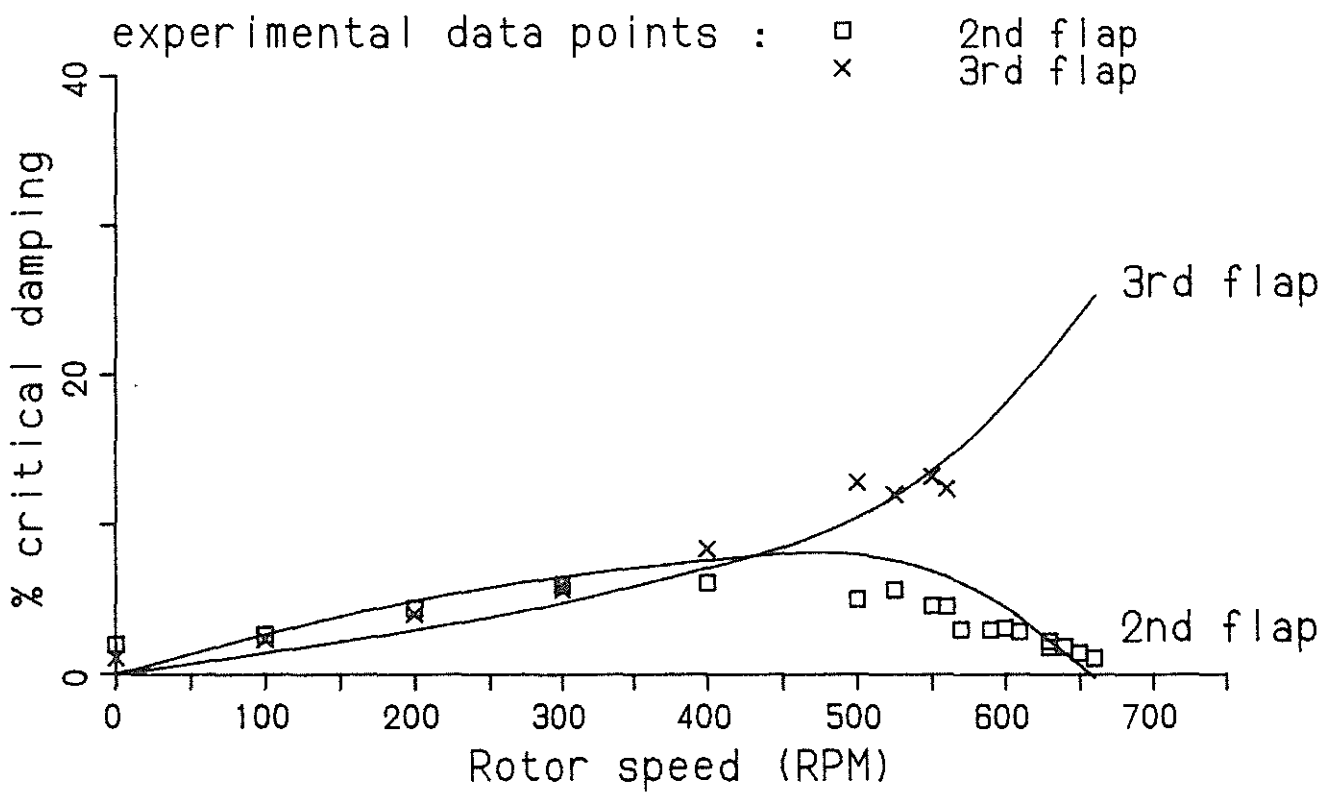
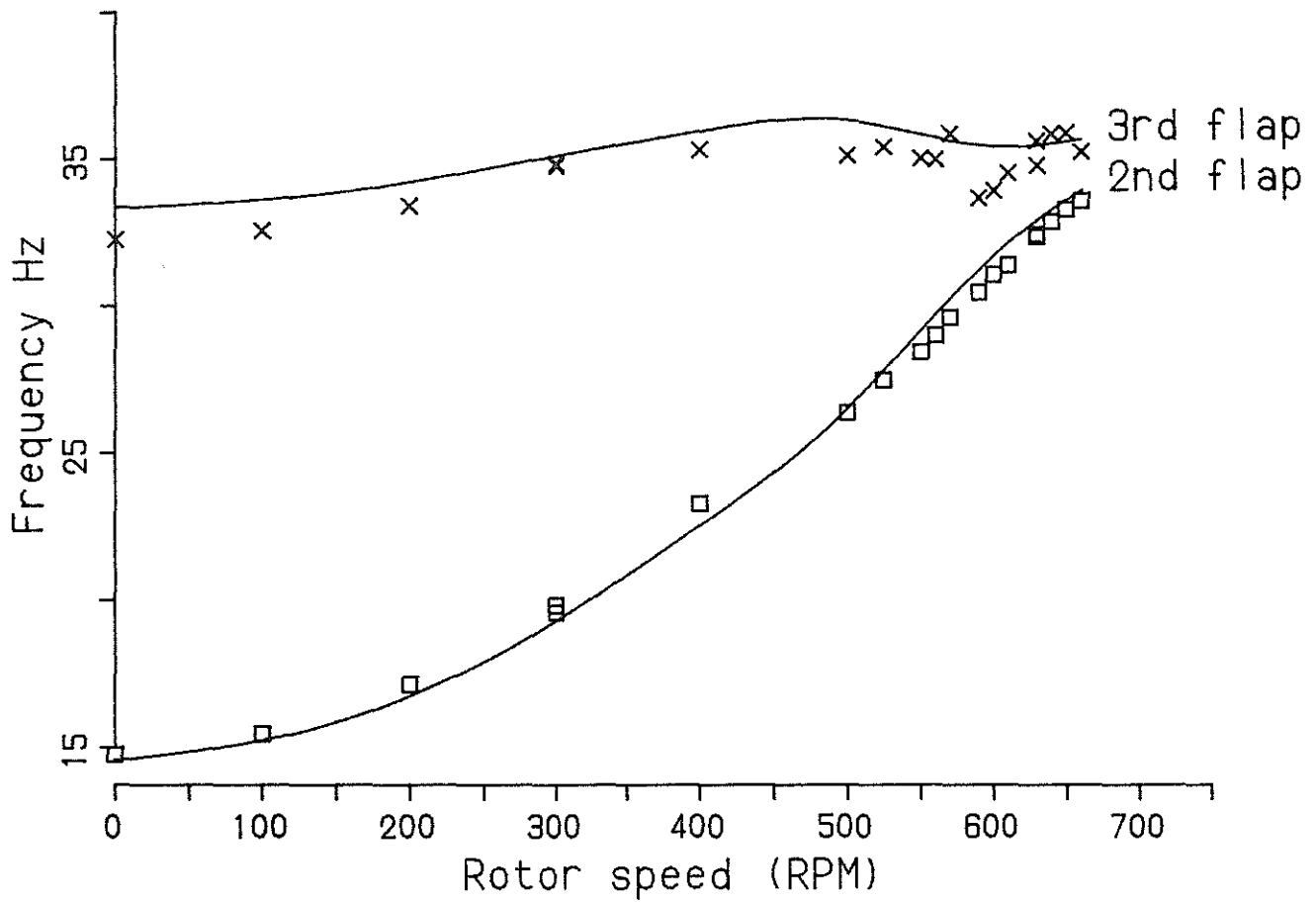


Fig 12    Modal frequencies and dampings for swept-tip blade with 120gm mass balance

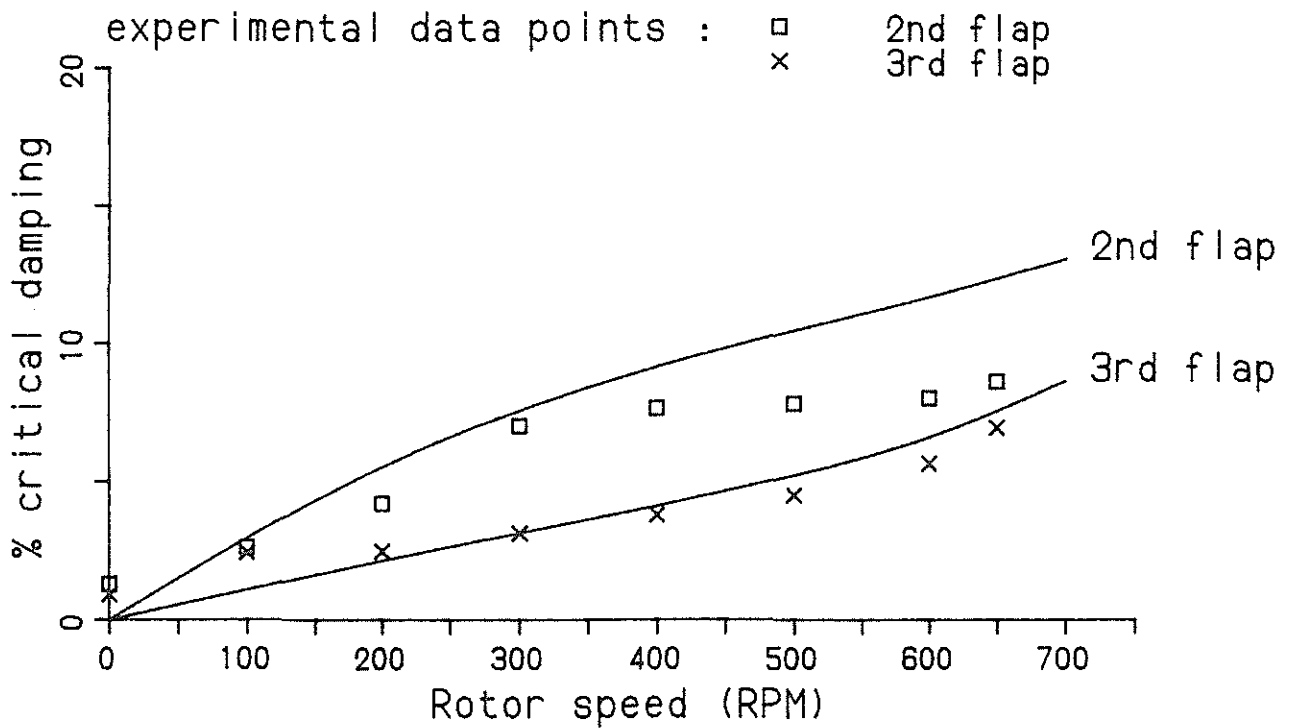
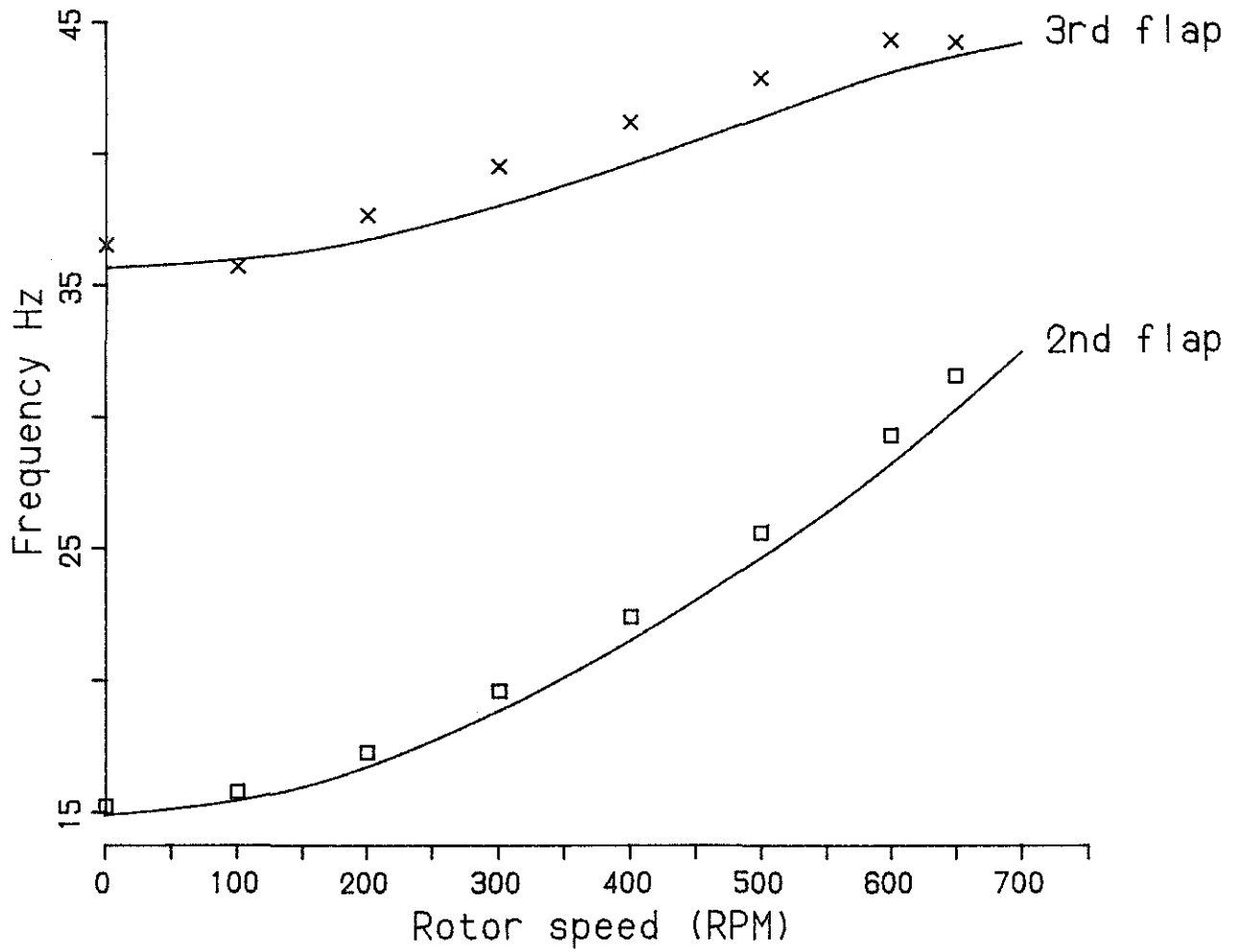


Fig 13 Modal frequencies and dampings for swept-tip blade with torsional stiffness doubled

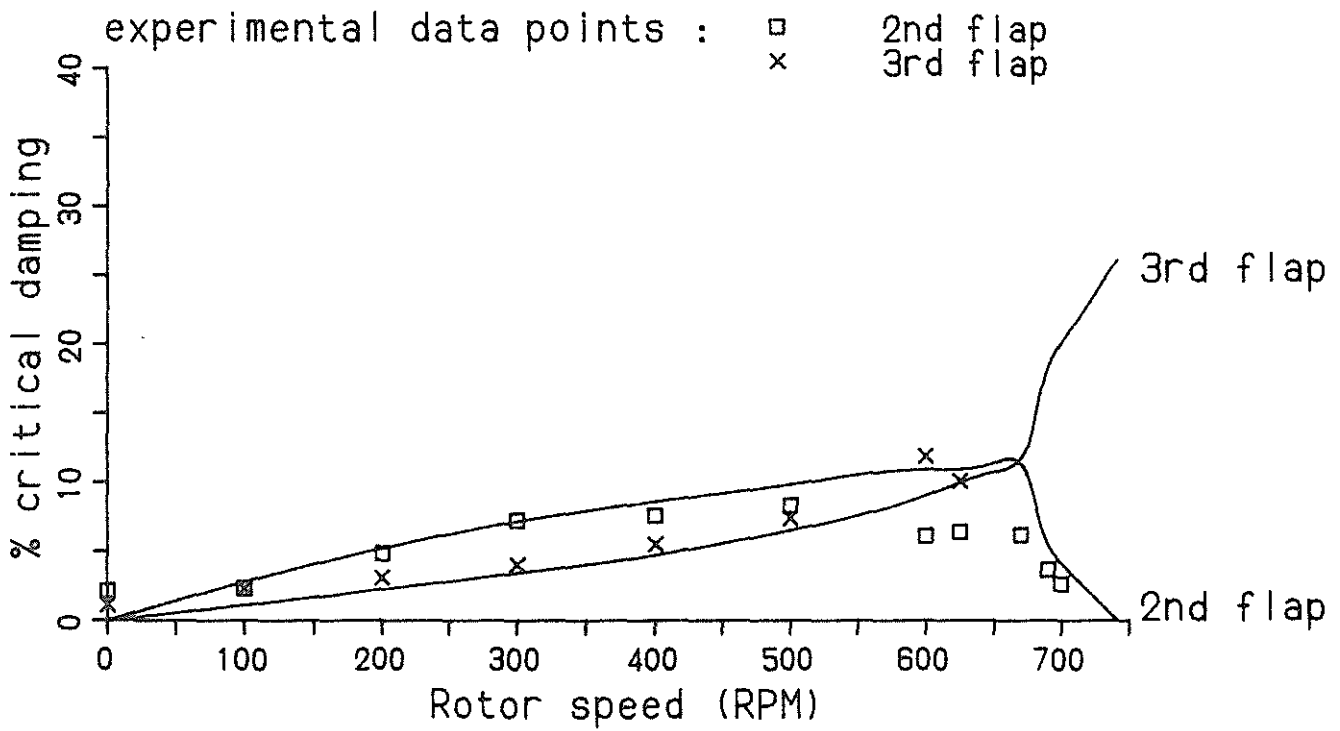
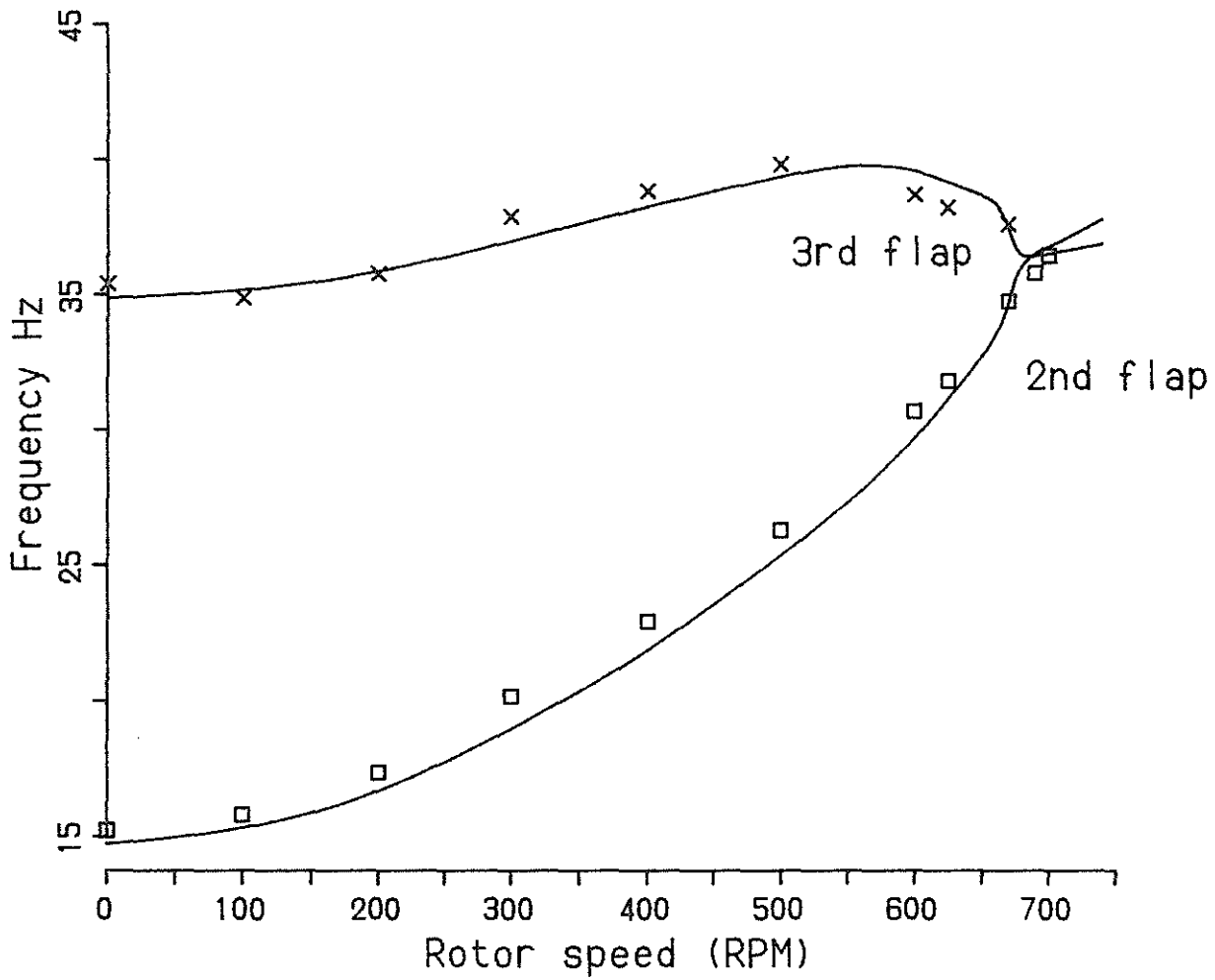


Fig 14 Modal frequencies and dampings for swept-tip blade with enhanced torsional stiffness and mass balance